Generating Compact, Guaranteed Passive Reduced-Order Models of 3-D RLC Interconnects

Nuno Alexandre Marques, Mattan Kamon, Luís Miguel Silveira, *Member, IEEE*, and Jacob K. White, *Member, IEEE*

Abstract—As very large scale integration (VLSI) circuit speeds and density continue to increase, the need to accurately model the effects of three-dimensional (3-D) interconnects has become essential for reliable chip and system design and verification. Since such models are commonly used inside standard circuit simulators for time or frequency domain computations, it is imperative that they be kept compact without compromising accuracy, and also retain relevant physical properties of the original system, such as passivity. In this paper, we describe an approach to generate accurate, compact, and guaranteed passive models of RLC interconnects and packaging structures. The procedure is based on a partial element equivalent circuit (PEEC)-like approach to modeling the impedance of interconnect structures accounting for both the charge accumulation on the surface of conductors and the current traveling in their interior. The resulting formulation, based on nodal or mixed nodal and mesh analysis, enables the application of existing model order reduction techniques. Compactness and passivity of the model are then ensured with a two-step reduction procedure where Krylov-subspace moment-matching methods are followed by a recently proposed, nearly optimal, passive truncated balanced realization-like algorithm. The proposed approach was used for extracting passive models for several industrial examples, whose accuracy was validated both in the frequency domain as well as against measured time-domain data.

Index Terms—Computational electromagnetics, coupled circuit-interconnect simulation, interconnect modeling, Krylov-subspace, model order reduction, packaging analysis, truncated balanced realization.

I. INTRODUCTION

AS VLSI circuit speeds and density continue to increase, the need for accurately modeling the effects of three-dimensional (3-D) interconnects has become essential for reliable chip and system design and verification. While measurement has always been an approach to model interconnects, in recent years much effort has been devoted to the fast and accurate computation of interconnect models directly from Maxwell's equations. For many portions of a design, the significant interconnect may be long and uniform enough to be modeled using a two-dimensional (2-D) approximation and transmission line theory. Unfortunately, discontinuities in this 2-D interconnect view, such as vias through planes, chip-to-board-connectors, and board-to-board connectors, require full 3-D modeling. To account for these, the designer, or CAD tool, must glue together 2-D and 3-D models which is cumbersome. Additionally, as circuit density increases, these discontinuities become more prevalent, and full 3-D modeling is the only course. Many of these structures are small compared to a wavelength, and therefore, retardation effects can be neglected when determining the coupling of dense interconnects. In that situation, an electromagneto-quasistatic (EMQS) approximation can be safely assumed. In the past decade, much work has been directed at rapidly solving for the inductance and capacitance of these structures [1], [2]. However, inductance and capacitance are not necessarily decoupled quantities, and for higher frequencies, a distributed model is necessary.

In this paper, we describe an integral equation approach to modeling the impedance of interconnect structures accounting for both the charge accumulation on the surface of conductors and the current traveling along conductors [3]–[5]. This formulation is very similar to the original standard Partial Element Equivalent Circuit (PEEC) technique that has long been used to model three dimensional interconnect structures [6]–[9]. The formulation can be solved with appropriate discretization resulting in an equivalent circuit representation. Nodal analysis or a mixed nodal-mesh approach are then used to formulate the circuit equations and to produce an impedance model of the interconnect structures under study. In order to simulate the interaction of these components with nonlinear circuit devices such as drivers and receivers, the resulting model must be incorporated into a time domain circuit simulator, such as SPICE or SPECTRE, in a suitable and efficient manner. When high accuracy is desired, however, these models can become excessively large and difficult to solve which precludes direct inclusion into a circuit simulator. In addition, due to full capacitive and inductive coupling, the circuit relations are dense, which quickly makes the problem computationally intractable. Compactness becomes, therefore, a critical issue, as much as the accuracy of the model itself.

The need for accurate, reduced-size, compact models leads us to consider model order reduction (MOR) techniques, which have been developed in the field of parasitic extraction [10]–[18]. For this reason, much work has been directed toward

N. Marques is with the Department of Mobile Communications, General Divison of Radio Communications, Alcatel Portugal, São Gabriel, Cascais, Portugal (e-mail: nuno.marques@alcatel.pt).

M. Kamon is with Coventor Inc., Cambridge, MA 02138 USA (e-mail: matt@coventor.com).

L. M. Silveira is with INESC ID/IST—Systems and Computers Engineering Institute R&D, the Department of Electrical and Computer Engineering, IST—Instituto Superior Técnico, Technical University of Lisbon, Lisbon, Portugal and also with Cadence Laboratories, Cadence Design Systems, Inc., San Jose, CA 95134 USA (e-mail: lms@inesc-id.pt).

J. K. White is with the Research Laboratory of Electronics, Department of Electrical Engineering and Computer Science, Massachusetts Institute of Technology, Cambridge, MA 02139 USA (e-mail: white@rle-vlsi.mit.edu).

generating reduced-order models *automatically* via moment matching or projection-based techniques [11], [15], [16], [19]. Since the interconnect structures are passive systems, i.e., they cannot produce energy internally, it is also necessary that the models generated also be passive, which implies stability as well. Otherwise, the models may cause nonphysical behavior when used in later simulations, such as by generating energy at high frequencies causing erratic or unstable time-domain behavior. Passive systems also enjoy another important property: Interconnected passive systems are also passive, while interconnected stable systems do not share such closure properties. In fact, interconnected stable systems are not even guaranteed stable (see [16] for an example).

Using standard MOR techniques, it is possible to generate guaranteed stable and passive reduced-order models for inclusion in circuit simulators such as SPICE. Additionally, such algorithms are ripe for acceleration techniques such as the Fast Multipole Method [1], [20] or the Precorrected-FFT [21] approach allowing the analysis of larger, more complex 3-D geometries. However, when models that accurately capture skin effect are needed, even these methods can generate models of too high an order for practical purposes [4], [5], [22]. Such a difficulty still precludes the use of such models in simulations since the model evaluation becomes too expensive. Furthermore, the poor performance of the moment matching approaches is surprising since the change in impedance due to skin effect is relatively smooth in many cases and one would expect a low-order model to capture such behavior very accurately. For this reason, other well-known methods in the control field have been examined, such as the method of truncated balanced realization (TBR), that is known to generate optimal or nearly optimal reduced-order state-space models [23]–[25]. An issue with the TBR-type methods that has prevented its widespread acceptance is that they cannot be relied on to preserve passivity. The techniques in [26] and [27] use a passivity-preserving initial reduction, but follow this reduction with a standard TBR method, and no means are given in either work to determine if the final model is passive or not. Recently, it has been shown that for the case of resistance–capacitance (*RC*) or resistance–inductance (*RL*) circuits, the TBR procedure does indeed produce provably passive reduced-order models [28]. This property was not however extended to RLC circuits.

In this paper, we describe a MOR technique based on a two-step procedure that combines a Krylov-subspace moment-matching method together with a recently proposed, nearly optimal, passive truncated balanced realization-like algorithm [28] to efficiently generate stable, passive and accurate, nearly optimal, reduced-order models of circuit interconnects. While this type of two-step procedure had previously been shown to produce good results, from a compactness standpoint, for inductance computations [26], as well as for RLC interconnects [27], our proposed method is, to our knowledge, the first one to enable efficient generation of accurate, compact, **guaranteed passive** reduced-order models of 3-D RLC interconnects, which is a nontrivial extension.

We begin in Section II by describing the PEEC-like integral formulation and discretization from which we derive the large dense linear system describing the interconnect structure. The issue of model compactness is discussed in Section III. We first describe a modified nodal analysis-based formulation that allows the direct application of MOR techniques to directly generate passive reduced-order models. This formulation is compared with a purely mesh-based counterpart, and an extension based on a combination of nodal and mesh analysis is also proposed that can be used to accelerate model construction. Then, the method of truncated balanced realizations and the new positive-real TBR-like (PR-TBR) approach are briefly reviewed, and its application to further compact the model is discussed. In Section IV, we apply the proposed algorithm to several example structures and establish a comparison in terms of compactness, i.e., model order, between the unreduced (full) models and the models obtained with the one-step reduction and the two-step process (including positive-real truncated balanced realization). The examples demonstrate that accurate and compact reduced-order models can be achieved through the use of our two-step reduction process and also exemplify the type of problems encountered with the traditional one-step reduction methods. Finally, conclusions are drawn in Section V.

II. MATHEMATICAL FORMULATION

A. Electromagnetic Formulation

Parasitic extraction for a set of conductors involves determining the relation between the terminal (or port) currents and the terminal voltages. Given a structure of k terminal pairs, the admittance matrix which relates the terminal currents and the terminal voltages is defined as $\boldsymbol{Y}_t(\omega)$ such that

$$\boldsymbol{Y}_t(\omega)\boldsymbol{V}_t(\omega) = \boldsymbol{I}_t(\omega) \qquad (1)$$

where sinusoidal steady-state at frequency ω is assumed. $\boldsymbol{Y}_t(\omega) \in \mathbb{C}^{k \times k}$ and $\boldsymbol{I}_t(\omega), \boldsymbol{V}_t(\omega) \in \mathbb{C}^k$ are the terminal current and voltage vectors, respectively [29]. If it is possible to compute the currents given the voltages at the terminals, then by adding voltage sources to all terminals in the circuit, $\boldsymbol{Y}_t(\omega)$ can be computed one column at a time. To do this, we set entry i of $\boldsymbol{V}_t(\omega)$ to one, the others to zero, and solve for $\boldsymbol{I}_t(\omega)$, which will be the ith column of $\boldsymbol{Y}_t(\omega)$.

To derive a relation between voltages and currents, we assume the quasistatic approximation and resort to an integral equation approach derived directly from Maxwell's equations and quite similar to the Partial Element Equivalent Circuit (PEEC) method [6]. At each point inside the conductors, we have

$$\boldsymbol{E} = -\nabla\varphi - \frac{\partial\boldsymbol{\Phi}}{\partial t} \qquad (2)$$

where

$$\varphi(\boldsymbol{r},t) = \frac{1}{4\pi\epsilon}\int_{V'}\frac{\rho(\boldsymbol{r}',t)}{\|\boldsymbol{r}-\boldsymbol{r}'\|}\,dv' \qquad (3)$$

$$\boldsymbol{\Phi}(\boldsymbol{r},t) = \frac{\mu}{4\pi}\int_{V'}\frac{\boldsymbol{J}(\boldsymbol{r}',t)}{\|\boldsymbol{r}-\boldsymbol{r}'\|}\,dv' \qquad (4)$$

$$\nabla\cdot\boldsymbol{J}(\boldsymbol{r},t) = -\frac{\partial\rho(\boldsymbol{r},t)}{\partial t} \qquad (5)$$

where $\boldsymbol{E}$ is the electric field, φ and $\boldsymbol{\Phi}$ are, respectively, the scalar and vector potentials, ϵ and μ are the electric permittivity and the magnetic permeability of the medium, respectively, V' is
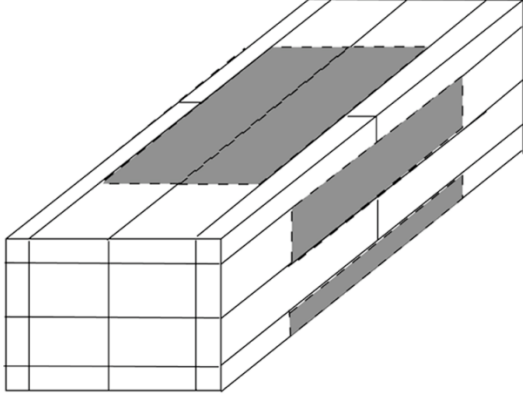
Fig. 1. Results of discretization operation applied to a conductor showing volume filaments (with its cross section decreasing toward the surfaces to properly capture skin and proximity effects) and charge panels (only some panels are shown).

the volume of all conductors, ρ is the charge density, and $\boldsymbol{J}$ is the current density. As mentioned, in deriving (3) and (4), the EMQS assumption was considered. So, our model will be valid only for structures small compared to a wavelength (in practice, one can accurately analyze structures on the order of a wavelength, because the interaction terms where retardation time is significant correspond to weak coupling; see [3], App. A).

To compute a model from this formulation, a discretization operation is performed on the conductors. Following the PEEC approach, the interior of each conductor is divided into a grid of filaments where each filament is assumed to have a constant current density with the direction of its length, and the surfaces of the conductors are covered with panels, where each panel is assumed to have a constant charge density. For conductors that are very long and thin, we can assume that the current running along its length is much larger than the current running along the other two orthogonal directions. In those cases, a filament discretization along a single direction is performed. For planar conductors, the filament discretization must be performed along two coordinate directions, and for volume-like conductors, filaments are set along the three-coordinate directions. This discretization operation allows one to generate an equivalent electrical "circuit" made up of filaments and panels. Fig. 1 shows the discretization operation applied to a long and thin conductor (filaments along one direction only), and Fig. 2 shows the electrical circuit associated with it.

To generate the constitutive relations for these elements, we apply the Galerkin method to (2) after discretizing the equation (see [6] for details). A constitutive relation for the filaments is obtained in the form of

$$Z_L I_b^f \equiv (\boldsymbol{R} + j\omega \boldsymbol{L}) I_b^f = V_b^f \qquad (6)$$

where $\boldsymbol{I}_b^f \in \mathbb{C}^f$ is the vector of f filament currents, $\boldsymbol{R}$ is the $f \times f$ diagonal matrix of filament dc resistances, $\boldsymbol{L}$ is the $f \times f$ dense, symmetric positive semidefinite matrix of partial inductances, and $V_b^f = \boldsymbol{\Phi}_{n_1} - \boldsymbol{\Phi}_{n_2}$ is the vector of voltages given as the difference between the node potential $\boldsymbol{\Phi}_n$ at the two ends of the filament. For explicit expressions for $\boldsymbol{R}$ and $\boldsymbol{L}$, see [4] and [6]. The derivation outlined is essentially the original PEEC for-

mulation [6]. However, in the following, we make a minor conceptual change that will enable us to generate a model with the right properties for the ensuing reduction steps. In the original PEEC method, the coefficients of potential matrix $\boldsymbol{P}' \in \mathbb{R}^{n \times m}$ are defined relating node potentials (at the extremities of filaments) with surface cell charges $\boldsymbol{\Psi} = \boldsymbol{P}' \boldsymbol{q}_p$ (n being the number of nodes, m the number of surface cells, and $\boldsymbol{q}_p \in \mathbb{C}^p$ being the charge on each of the p panels). Then, using $\boldsymbol{P}'$, (3) is enforced on interior nodes. Note, however, that imposing the potential on internal nodes as an explicit function of the surface charges is equivalent to putting a voltage source on the nodes, which allows for fictitious current flow out of the node, which violates current conservation. In other words, even though an exact solution of the integral equation can be found that satisfies the Current Conservation Law (5) inside the conductors, the discretized system does not enforce this condition. In our formulation, we choose instead to enforce (5) explicitly. To that end, we write an equation involving $\boldsymbol{P} \in \mathbb{R}^{p \times p}$, which relates the panel charges with the node potentials, including both external nodes on conductor surfaces, where charges reside, and internal nodes. See [4] for the expression of $\boldsymbol{P}$. Note also that we allow multiple panels on each node—as is the case for nodes on edges or conductor corners. Furthermore, in our formulation, $\boldsymbol{P}$ is square, allowing us, as we shall see, to establish a set of equations, amenable to generate stable and passive reduced-order models.

Since the current flowing onto the panels is given by $\boldsymbol{I}_b^p = d\boldsymbol{q}_p/dt$, for the sinusoidal steady state, we can write $\boldsymbol{q}_p = \boldsymbol{I}_b^p/(j\omega)$. Additionally, since the panel node voltages are voltages relative to infinity, we can view the panel branches as connecting the panel node to the zero potential node at infinity. Then, the panel branch voltages are given by $\boldsymbol{V}_b^p = \boldsymbol{\Phi}_p - 0 = \boldsymbol{\Phi}_p$, where $\boldsymbol{\Phi}_p$ are the panel potentials. Combining, we get a relation between the panel currents and their voltages $\boldsymbol{V}_b^p = 1/j\omega\, \boldsymbol{P} \boldsymbol{I}_b^p$. With this relation and (6), we can write the constitutive relations for the elements as a single matrix in $\mathbb{C}^{b \times b}$, $b = f + p$

$$\boldsymbol{V}_b = \begin{bmatrix} \boldsymbol{V}_b^f \\ \boldsymbol{V}_b^p \end{bmatrix} = \begin{bmatrix} \boldsymbol{Z}_L & \boldsymbol{0} \\ \boldsymbol{0} & \boldsymbol{P}/(j\omega) \end{bmatrix} \begin{bmatrix} \boldsymbol{I}_b^f \\ \boldsymbol{I}_b^p \end{bmatrix} = \boldsymbol{Z} \boldsymbol{I}_b \qquad (7)$$

where $\boldsymbol{I}_b \in \mathbb{R}^b$ is the vector of branch (filaments plus panels) currents and $\boldsymbol{V}_b$ is the vector of branch (filaments plus panels) voltages. See Fig. 2 for an illustration of these quantities.

B. Model Generation

Applying voltage sources to the circuit, we can now solve it and extract the desired terminal currents, thus, producing the required admittance model. To that end, we will use a nodal analysis technique. As the model is expected to be used later for time-domain simulations, ensuring accuracy at dc is imperative. Since our model assumes zero-potential at infinity and only capacitors and sources connect to the zero-potential node, only voltage sources can be used in the computation. Kirchoff's Current Law, which enforces (5) at the nodes of the discretized system, requires that the sum of the branch currents leaving each node in the network must be zero. This can be written as

$$[\boldsymbol{D} \quad -\boldsymbol{N}] \begin{bmatrix} \boldsymbol{I}_b \\ \boldsymbol{I}_{\mathrm{src}} \end{bmatrix} = [\boldsymbol{0}] \qquad (8)$$
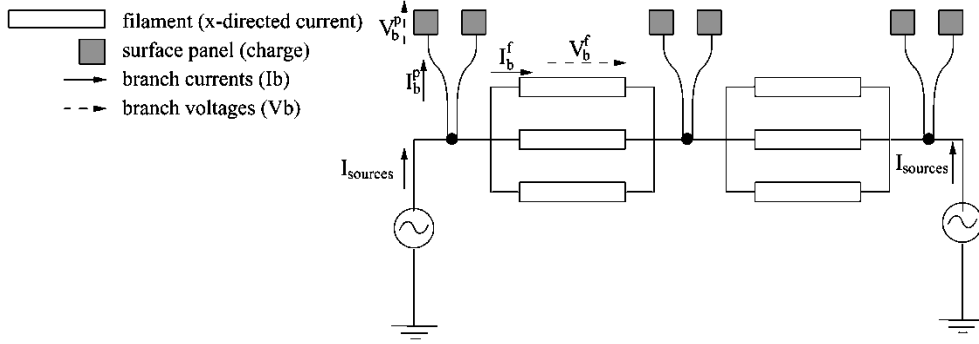
Fig. 2. Simplified version of the electrical circuit corresponding to the discretization shown in Fig. 1—nodal analysis quantities are described.

where $D \in \mathbb{R}^{n \times b}$ is the sparse nodal incidence matrix summing the filament and panel currents in each node, $N \in \mathbb{R}^{n \times n_{\mathrm{src}}}$ is the sparse matrix summing the currents through the voltage sources, n is the number of nodes (excluding the one for the point at infinity), b is the number of branches (filaments plus panels), and n_{src} is the number of voltage sources in the circuit. $I_{\mathrm{src}} \in \mathbb{R}^{n_{\mathrm{src}}}$ is the vector of currents leaving each voltage source (always connected to ground) and entering the terminal nodes. Note the $[0]$ in the right-hand side due to the absence of current sources in the circuit.

Applying Kirchoff's Voltage Law to the circuit, we obtain

$$\begin{bmatrix} D^T \\ N^T \end{bmatrix} [V_n] = \begin{bmatrix} V_b \\ V_{\mathrm{src}} \end{bmatrix} \qquad (9)$$

where V_n is the vector of voltages at each node in the network, and V_{src} are the known source voltages. Note that V_{src} is exactly the terminal voltage vector V_t, from (1). Combining (9) with (7) and (8) yields a model in the form of a system of equations in mixed node-branch form. One approach to coupling the above models with circuits is to directly include that model directly into a circuit simulator. This approach has the drawback that the size of such a model can easily be very large if high accuracy is desired. Even computing the admittance matrix directly, as described at the beginning of this section is inefficient, as it requires k solutions of a system with a very large matrix. The use of iterative methods could reduce the computational cost of solving this system. Still, the resulting model would be valid only at a single frequency. However, to design with this admittance model, it is often necessary to perform coupled simulation with nonlinear devices, such as CMOS drivers and receivers. Nonlinear devices require time domain simulation, and thus, the admittance information is necessary from dc up to the highest frequency of interest in the circuit. Thus, it is essential to have models valid for a continuous range of frequencies. It is possible to perform the above computations for a number of frequencies and then use some interpolating technique to compute a model valid over that range [30]–[32]. While recent work has indeed made it possible to compute passive, arbitrarily accurate (i.e., high order) interpolants of frequency described subsystems [32], [33], the extremely high cost of solving for each frequency point will, in general, preclude such a methodology. Instead, more efficient techniques have to be sought. To that end, we turn to MOR techniques.

III. MODEL ORDER REDUCTION

MOR methods are well known in the control theory and linear algebra areas. They have more recently been applied with success to linear systems in computer-aided design, specifically interconnect modeling, and have seen considerable and steady progress in the past few years [10], [11], [15], [16]. Moment matching and the more general projection-based techniques [11], [15], [16], [19], have been applied in order to *automatically* generate reduced-order models of electromagnetic couplings in interconnect and packaging structures [12], [15]. Algorithms, such as passive reduced-order interconnect macromodeling algorithm (PRIMA) [16], have been presented that produce guaranteed stable and passive reduced-order models. Such methods, which rely on simple algebraic operations, are extremely efficient and able to accurately capture the relevant behavior of the underlying systems. PRIMA-type algorithms or their multipoint variants [17] have thus become the method of choice for MOR and an essential component of any interconnect and packaging modeling strategy.

The basic idea behind MOR techniques is to reduce the size of the system described by the circuit equations to a much smaller one that still captures the dominant behavior of the original system. If the circuit equations are written in the state-space form

$$s\mathcal{L}x = -\mathcal{R}x + \mathcal{B}u$$
$$y = \mathcal{B}^T x. \qquad (10)$$

where $s = j\omega, \mathcal{L}, \mathcal{R} \in \mathbb{R}^{N \times N}, \mathcal{B} \in \mathbb{R}^{N \times k}, x \in \mathbb{R}^N$ is the state vector, $y \in \mathbb{R}^k$ the output, $u \in \mathbb{R}^k$ the input, N the size of the original model, and k the number of terminals considered, then MOR aims at obtaining a reduced model

$$s\tilde{\mathcal{L}}\tilde{x} = -\tilde{\mathcal{R}}\tilde{x} + \tilde{\mathcal{B}}u$$
$$y = \tilde{\mathcal{B}}^T \tilde{x} \qquad (11)$$

where $\tilde{\mathcal{L}}, \tilde{\mathcal{R}} \in \mathbb{R}^{r \times r}, \tilde{\mathcal{B}} \in \mathbb{R}^{r \times k}, \tilde{x} \in \mathbb{R}^r$ is the reduced-order state vector, and $r \ll N$ is the order of the reduced model and such that (11) is a good approximate to (10) in some appropriate norm.

Since the interconnect structures are passive systems, it is desired that the reduced models produced also be passive. Otherwise, the models may cause nonphysical behavior when used

in later simulations, such as by generating energy at high frequencies that causes erratic or unstable time-domain behavior. It is known [16] that a sufficient condition for generating stable and passive reduced-order models is that both $(\mathcal{R} + \mathcal{R}^T)$ and $(\mathcal{L} + \mathcal{L}^T)$ be positive semidefinite.

However, when models are needed which accurately capture skin effect, even these methods can generate models of too high order for practical purposes [4], [5], [22]. In such cases, reduction algorithms such as PRIMA generate models with a large number of small real poles. These poles are selected during the reduction due to their closeness to the expansion point (zero or infinity). As we shall see in Section IV, examination of the residues associated with such poles shows that they have a negligible effect on the system behavior and should in fact be discarded. This high order precludes the use of such models in circuit simulation since the model evaluation steps becomes too expensive. For this reason, other well-known methods in the control field, such as the method of TBR, that are known to generate optimal or nearly optimal reduced-order state-space models [23]–[25] have gained renewed interest. Historically, two issues have prevented the widespread use of TBR-type methods for parasitic extraction: their high computational cost and the lack of guarantees of passivity for the resulting models. In fact, computation of the TBR model requires a full symmetric eigendecomposition of the system matrix and therefore has a cost that is cubic in the size of the system. As such, it cannot be used as a reduction algorithm for large systems. However, the initial application of an algorithm such as PRIMA can reduce a large model with tens of thousands of unknowns to a reduced model on the order of a few hundreds to a thousand. Application of a TBR-like method to such a reduced model is thus acceptable from a computational standpoint. Furthermore, recently, a positive-real TBR-like algorithm was proposed that is shown to generate nearly optimal, passive, and accurate, reduced-order models of circuit interconnects [28]. Like TBR, this method is computationally too expensive to be applied directly to our original model but is acceptable if applied after some initial reduction is performed.

Therefore, our proposed model reduction approach is a hybrid, two-step, procedure that combines a Krylov-subspace moment-matching method followed by the positive-real balanced truncation algorithm. The *rationale* behind this procedure is to take advantage of the computational efficiency of the Krylov-type methods to reduce the original system down to a size for which application of the balancing transformation is amenable. In the next section, we describe the formulation of the circuit equations enabling the application of the PRIMA algorithm for an initial reduction, and in Section III-B, we describe the application of the positive-real balanced truncation procedure. Since these techniques are fairly standard and have been well described elsewhere, we only summarize their main features.

A. Krylov-Subspace-Based Passive Model Order Reduction

To derive a state space admittance model the powers of the Laplace variable $s = j\omega$ must all be to the first power only. However, the constitutive relation Z in (7) contains terms with both s and $1/s$. To separate the $1/s$ power, the branch currents

can be separated into two types: $I_b = [I_b^f; I_b^p]$, where I_b^f represents the currents in filaments, and I_b^p represents the currents onto panels. Also, the nodal incidence matrix, D is split into $[A, B]$, where A sums filament currents and B sums panel currents. Moreover, each of these matrices is further split considering separately external nodes (subscript e) and internal nodes (subscript i). An internal node is a node to which no panels are connected. Consequently, $A = [A_e; A_i]$, where A_e corresponds to the n_e external nodes and A_i corresponds to the n_i internal nodes. A similar procedure can be applied to B. Equation (9) can also be rewritten, separating the branch voltages in $V_b = [V_b^f; V_b^p]$. V_n^e and V_n^i correspond to, respectively, the voltage in external and internal nodes. Putting it all together, the desired state-space form is obtained (see [4] for the full derivation)

$$
s \begin{bmatrix} L & 0 & 0 & 0 \\ 0 & B_e P^{-1} B_e^T & 0 & 0 \\ 0 & 0 & 0 & 0 \\ 0 & 0 & 0 & 0 \end{bmatrix} \begin{bmatrix} I_b^f \\ V_n^e \\ V_n^i \\ I_{\mathrm{src}} \end{bmatrix}
$$
$$
= - \begin{bmatrix} R & -A_e^T & -A_i^T & 0 \\ A_e & 0 & 0 & -N_e \\ A_i & 0 & 0 & 0 \\ 0 & N_e^T & 0 & 0 \end{bmatrix} \begin{bmatrix} I_b^f \\ V_n^e \\ V_n^i \\ I_{\mathrm{src}} \end{bmatrix} + \begin{bmatrix} 0 \\ 0 \\ 0 \\ V_{\mathrm{src}} \end{bmatrix} \quad (12)
$$

which can readily be written as (10). It was shown in [4] that this system satisfies the necessary requirements for generation of guaranteed passive reduced-order models. MOR techniques can thus be applied directly to this formulation. Note that, as detailed in [5], this formulation has advantages in terms of model sizes over the one developed in [34] using mesh analysis, for similar accuracy. In fact, the number of states in the nodal case is $f + n + n_{\mathrm{src}}$, while for the mesh formulation, it is $f + 2p - n$ (f being the number of filaments, n the number of nodes, n_{src} the number of sources, and p the number of panels). Thus, the nodal formulation is more efficient where $p > n$, which is always the case for discretizations along one or two directions.

An additional advantage of the nodal formulation is the ability to perform expansions around any point in the complex plane, including $s = \infty$, given the added flexibility that it provides. For expansions around $s = \infty$, the matrix $\mathcal{L}$ from (10) will require inversion. Unlike mesh analysis, in the nodal formulation, as seen in (12), $\mathcal{L}$ is nonsingular if there are no internal nodes, which is a common situation in long and thin conductors. The derivation of such a model is discussed in [5] and [35]. Computing a reduced-order model from (10) with an algorithm such as PRIMA, using any expansion point, corresponds to solving a linear system with a matrix that involves $\mathcal{R}$ and $\mathcal{L}$ in some form. If $s = 0$ is considered, then the system matrix is $\mathcal{R}^{-1}\mathcal{L}$. In the case $s = \infty$ presented above, $\mathcal{L}^{-1}$ is required to form the system matrix $\mathcal{L}^{-1}\mathcal{R}$. In practice, $\mathcal{L}$ is never inverted explicitly: If $\mathcal{L}^{-1}b = x$ is needed, $\mathcal{L}x = b$ is solved for x using an iterative algorithm such as generalized minimal residual (GMRES) [36].

The form of the $\mathcal{L}$ matrix reveals one of the differences between the nodal and mesh formulations. In the latter, the block matrices describing the filament constitutive relations appear together with the mesh matrix M, leading to the existence of a block such as MLM^T in $\mathcal{L}$ (see for instance [34]), while in

the former, L is used directly, as shown in (12). It is known that under an appropriate choice of preconditioner, the condition number of a system obtained from the matrix MLM^T can be *significantly smaller* than that obtained from the partial inductance matrix L (see [37] for a proof). Thus, a faster system solution using $\mathcal{L}$ can be accomplished in the nodal formulation if the block L were replaced by a term like MLM^T in $\mathcal{L}$, as in the mesh formulation. Such a substitution implies the combination of a mixed nodal and mesh analysis method taking advantage of the best characteristics of each system.

This can be accomplished by replacing the filament branch currents in (12) as unknowns by a set of mesh currents covering all filaments I_m^f. For the complete formulation, see [5], and [35]. In this mixed formulation, again, both the resulting $\mathcal{R}$ and $\mathcal{L}$ matrices satisfy the conditions required for passive MOR, and the size of the system is the same as that of the nodal formulation. Also, as for nodal, $\mathcal{R}$ and $\mathcal{L}$ (subjected to the same thin conductor restrictions) are nonsingular, meaning that any expansion point can be used in the model order reduction.

B. Positive-Real Truncated Balanced Order Reduction

Applying PRIMA to an Nth-order system described by (12) leads to a smaller system (11) of order $r \ll N$, with a similar form but involving reduced system matrices $\tilde{\mathcal{L}}$, $\tilde{\mathcal{R}}$, and $\tilde{\mathcal{B}}$. This realization can also be written in standard form as

$$\dot{x} = Ax + BV_t$$
$$I_t = C^T x + DV_t \tag{13}$$

where $A = -\tilde{\mathcal{L}}^{-1}\tilde{\mathcal{R}}, B = \tilde{\mathcal{L}}^{-1}\tilde{\mathcal{B}}, C = \tilde{\mathcal{B}}$, and x is the vector of internal state variables. Here, we have generalized the formulation by adding a direct term D to the equations. Typically, $D = 0$, but in the following, we will see that D does play a role in the reduction. To further reduce the system, we seek to find an even smaller representation $[\hat{A}, \hat{B}, \hat{C}, \hat{D}]$ of size $q \ll r$, which maintains the overall accuracy of the original model. An obvious choice is spectral truncation, which is based on computing an eigendecomposition of the system matrix and truncating it, is unlikely to produce accurate models, as it will favor the low-frequency content of the system. Thus, it will potentially tend to keep the "weak" low-frequency poles that we know are not relevant, while discarding some high-frequency poles that are likely to be important to the system behavior. Instead, what is required is a method that can explicitly indicate which modes contribute the most to the system response. The methods of TBR [23] and Hankel Norm Approximation [24] have long been used in the control systems literature to address such a problem. The TBR algorithm performs a coordinate transformation such that the system states are ordered in terms of their contribution to the system response from an input–output standpoint. In essence, the transformation computes a measure of how *controllable* a given state is from the input and how *observable* a state is at the output. States which are both weakly observable (i.e., produce free evolution outputs with small norm) and weakly controllable (i.e., require large inputs to be reached) do not contribute to the frequency response and can be discarded or truncated.

In order to compute a TBR reduced-order model, the system must first be internally balanced. A coordinate transformation T is computed, and a change of state variables $\hat{x} = Tx$ is performed in order to obtain a "balanced" realization of (13) from an input–output standpoint. This transformation is determined from the controllability and observability grammians W_c and W_o, which are the solutions of the Lyapunov equations

$$AW_c + W_c A^T = -BB^T$$
$$A^T W_o + W_o A = -C^T C. \tag{14}$$

Under a similarity transformation of the state-space model

$$A \to T^{-1}AT, \quad B \to T^{-1}B, \quad C \to CT \tag{15}$$

the input–output properties of state-space model, such as the transfer function, are invariant (only the internal variables are changed). The grammians, however, are not invariant, but the eigenvalues of the product $W_c W_o$ are easily seen to be invariant. These eigenvalues, the Hankel singular values, contain useful information about the input–output behavior of the system. In particular, "small" eigenvalues of $W_c W_o$ correspond to internal subsystems that have a weak effect on the input–output behavior of the system and are, therefore, close to nonobservable or noncontrollable or both. For a full description of the algorithm, see [23] and [24]. The similarity transformation T is thus chosen such that it leaves the state-space system dynamics unchanged but makes the (transformed) grammians equal and diagonal. Furthermore, the diagonal entries of these grammians $\hat{W}_{c_{ii}} = \hat{W}_{o_{ii}} = \sigma_i$, where $\sigma_1 \geq \sigma_2 \geq \cdots \geq \sigma_N > 0$, are the Hankel singular values and a measure of the controllability and observability of each state. If the state variables $\hat{x}$ are ordered such that $\sigma_i > \sigma_{i-1}$, then the realization can be partitioned as

$$\begin{bmatrix} \dot{\hat{x}}_1 \\ \dot{\hat{x}}_2 \end{bmatrix} = \begin{bmatrix} \hat{A}_{11} & \hat{A}_{12} \\ \hat{A}_{21} & \hat{A}_{22} \end{bmatrix} \begin{bmatrix} \hat{x}_1 \\ \hat{x}_2 \end{bmatrix} + \begin{bmatrix} \hat{B}_1 \\ \hat{B}_2 \end{bmatrix} V_t$$
$$I_t = [\hat{C}_1 \quad \hat{C}_2] \begin{bmatrix} \hat{x}_1 \\ \hat{x}_2 \end{bmatrix} + DV_t \tag{16}$$

where the weakly controllable and observable modes are given by $\hat{x}_2$ and the desired reduced-order model is represented by $[\hat{A}_{11}, \hat{B}_1, \hat{C}_1, D]$ [23]. Most importantly, it has been shown that for a truncation of order q, the error between the original and reduced models satisfies

$$\|E_q(s)\|_{L_\infty} = \left\| Y_t(s) - Y_t^{(q)}(s) \right\|_{L_\infty} \leq 2(\sigma_{q+1} + \cdots + \sigma_N) \tag{17}$$

where, again assuming an admittance representation for the system, $Y_t^{(q)}$ is the qth-order reduced model, and L_∞ corresponds to the maximum norm over all s. The existance of an approximation error bound is a feature unavailable to Krylov-subspace methods. In addition, if the original system is stable, which we know to be the case here, so is the truncated system. Furthermore, the guarantee of monotonicity of the error in (17) allows us to choose a higher order model until the

error is adequate. Note that since the Hankel singular values are all computed in the balancing transformation, no additional computation is necessary to raise the order of the model.

The main drawback of the TBR method is that passivity of the resulting model cannot be guaranteed. In making assessments about passivity, we require a tool that can assess the positive-realness of a state-space model in a global manner. One such tool is the positive-real lemma [38], which states that a system in the form of (13) is positive-real if and only if there exist matrices $X_c = X_c^T, J_c, K_c$ such that the Lur'e equations

$$AX_c + X_cA^T = -K_cK_c^T \quad (18)$$

$$X_cC^T - B = -K_cJ_c^T \quad (19)$$

$$J_cJ_c^T = D + D^T \quad (20)$$

are satisfied, and $X_c > 0$ (i.e., X_c is positive semi-definite). X_c is analogous to the controllability grammian W_c discussed above. In fact, it is the controllability grammian for a system with the input-to-state mapping given by the matrix K_c. It should not be surprising that there is a dual set of Lur'e equations for $X_o = X_o^T > 0, J_o, K_o$ that are obtained from (18)–(20) by the substitutions $A \rightarrow A^T, B \rightarrow C^T$, and $C^T \rightarrow B$, and which is naturally related to the observability grammian W_o. It is easy to verify that X_c, X_o behave, under similarity transformation, just as W_c, W_o, that their eigenvalues are invariant, and in fact in most respects they behave as the grammians W_c, W_o.

A passivity-preserving reduction procedure follows readily by noting that the Lur'e equations can be solved for the quantities X_c, X_o which may then be used as the basis for a TBR procedure, i.e., to determine T. We may thus find a coordinate system in which $\hat{X}_c$ and $\hat{X}_o$ are equal and diagonal. In this coordinate system, the system matrices may be partitioned and truncated, just as for the standard TBR procedure, to give the reduced-model defined by $[\hat{A}, \hat{B}, \hat{C}, \hat{D}]$. Such a reduced-order system is easily proven to be guaranteed passive. For details, see [28]. Similarly to the TBR-like methods, the procedure described also has computable error bounds, albeit their interpretation is not as simple as that of (17). Furthermore, the bound and the reduction algorithm are slightly more complicated if $D = 0$. In this case, one solution that seems to work well is to perturb the system slightly by adding a small direct term D, perform the reduction, and then extract the perturbation, since it is a direct term. If the perturbation is kept small, the error incurred is minimal and can generally be discarded. For a presentation of the error bound, again, see [28].

While the error bound is not so easily understood, the physical interpretations is actually fairly simple. According to [28], the positive-real TBR algorithm balances the importance of past energy inputs and future energy outputs. This is achieved by transforming to a coordinate system in which X_o and X_c are equal and diagonal and in which the invariant quantities that are the eigenvalues of the product of X_o and X_c are easily calculated. The algorithm will keep in the final reduced-model only modes that are either energy-wise, easily controllable, or observable,
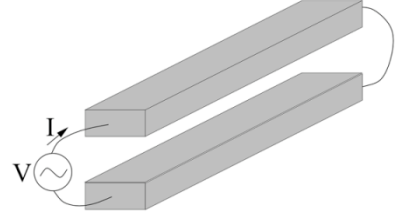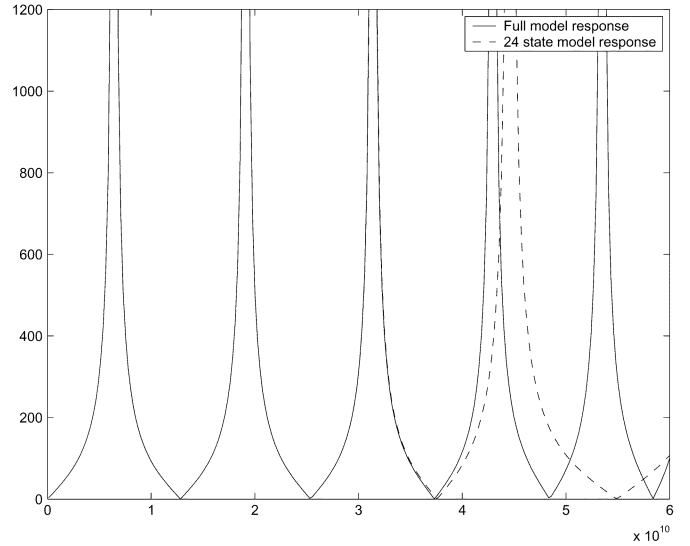

Fig. 3.   Two-conductor example.

Fig. 4.   Results obtained for a simple geometry without appropriately modeling skin effect (case A). Comparisons are made between the full model and a 24th-order model computed using PRIMA.

that is, they do not need much energy input to be reached, or it is possible to extract a lot of energy from them. This was exactly our goal for this reduction step, namely, to keep all modes which have relevant energy content from an input–output standpoint.

IV. RESULTS

A. Simple Two-Conductor Example

For our first example, we consider a very simple geometry made up of two long and thin conductors, as shown in Fig. 3. It is easy to see that, for this structure, the dominant behavior is similar to a transmission line. In our example, both conductors are 1 cm long, 37 μm wide, 13 μm in height, and separated by 17 μm. A simple discretization (let us call it "case A") is first applied to this geometry dividing each conductor in ten segments, where each segment is filled with only one filament. Four hundred sixteen panels cover all surfaces. Using our nodal formulation, this results in a system with 43 states. Fig. 4 shows the frequency response of the input impedance, for the full system and for a 24th-order reduced model, computed using the PRIMA algorithm around $s_0 = 0$. Note that since the structure is 1 cm long, and considering the quasistatic assumption, the model is valid for frequencies up to 30 GHz (for which the wavelength is 1 cm). It is usually considered that the valid range of frequencies is up to one tenth of this value, but in practice this value can be assumed (see [3], App. A). A larger band is shown on
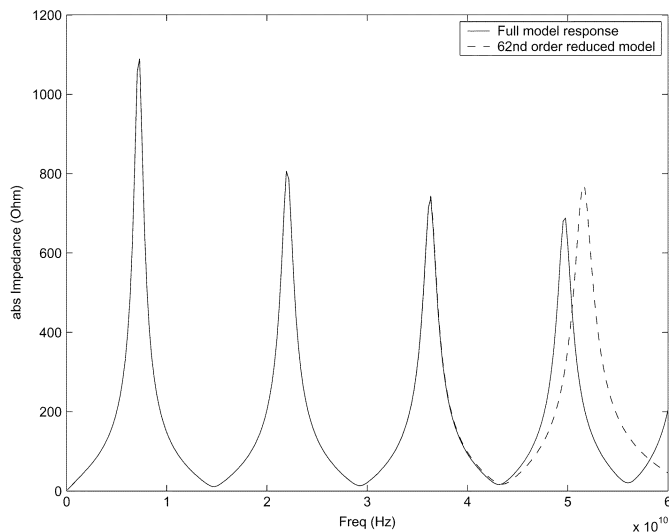
Fig. 5.   Impedance frequency response results obtained for a simple geometry when skin effect is modeled (case B). Comparisons are made between the full model and a 62nd-order reduced model computed using PRIMA.

the figure to clearly show the frequency behavior of the approximated model with the MOR technique. From the figure, one can see that the reduced model is extremely accurate in the frequency range for which the approximation is valid.

Consider now a different discretization of the same structure ("case B") where each segment of each conductor is now filled with 15 filaments, while the number of panels remains the same. Filaments are chosen to be smaller near the edges so that its width is equal to the skin depth. The full system in this case has now 323 states. Fig. 5 presents results similar to those of the previous case and shows that a 62nd-order reduced model is necessary in order to accurately match the same three first resonances. Note that the differences in the amplitudes of the peaks in the full system frequency responses are due to the skin effect, which was not modeled in case A. One would expect that the similar dominant behavior of both cases would be similarly captured using a reduced-order of approximately the same order. However, that does not seem to be the case as had previously been reported [4], [5], [22]. This example illustrates the difficulties that Krylov-subspace algorithms have in compacting models resulting from PEEC-like discretizations, namely those involving volume discretizations.

To understand this, we considered the pole distributions in both cases. In case B, as depicted in Fig. 6(a), there is a large number of purely real poles, something that does not happen in case A. By noting the scale of the plot, many of these real poles are closer to the origin than the vertically aligned poles that are common to both figures. It is known that Krylov-subspace type algorithms behave in a manner such that when the order of the approximation is increased, they proceed by matching poles or clusters of poles as determined by their closeness to the expansion point [39]. This explains why a 62nd-order model is obtained, despite the fact that almost all of the poles matched are not very relevant. This fact can be verified by inspection of Fig. 6(b), which shows the residues resulting from a pole-residue decomposition performed on the full system (case B). The poles with higher residues correspond to those poles also
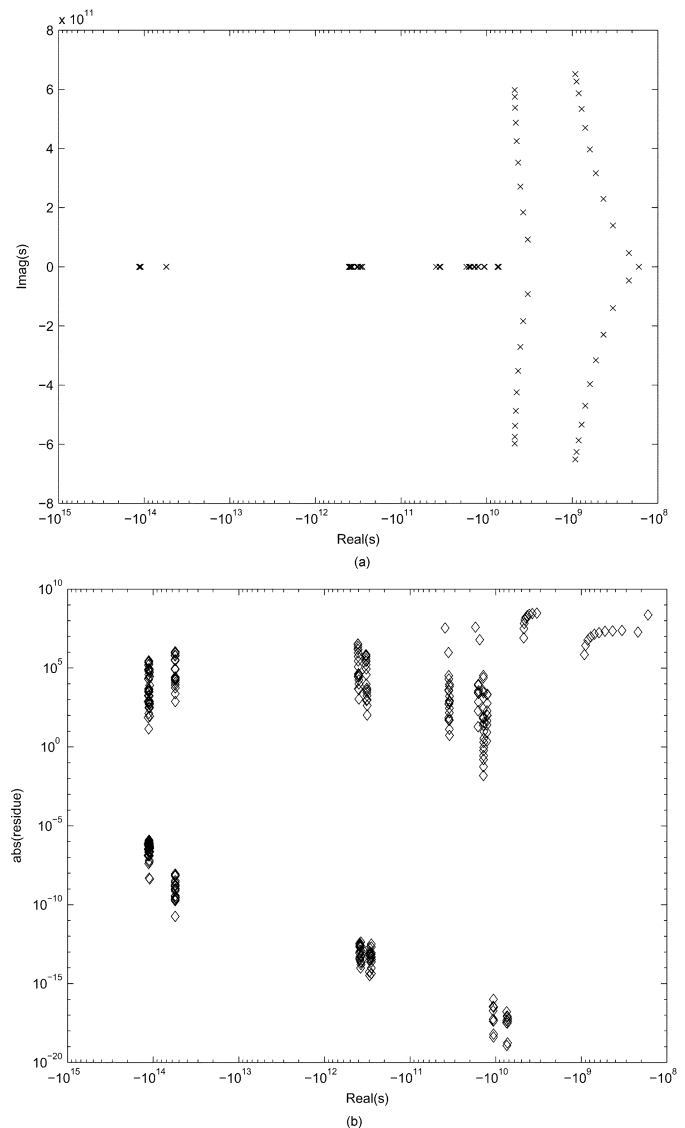

Fig. 6.   Pole-residue decomposition of the 323rd-order full system obtained for the simple geometry by applying the nodal formulation, when skin effect is modeled (case B). (a) Poles distribution and (b) its corresponding residues. Note that the abscissa axis is the same in both figures.

present in the system not modeling skin effect (case A). These nondominant poles, which appear in clusters in the real axis, are responsible for the large orders required for the reduced models shown, since the MOR algorithm has to capture all or part of these clustered poles before reaching an acceptable number of dominant poles. The distribution of these nondominant poles and this particular behavior of the MOR algorithm is common to all the PEEC-like circuits we have tried when skin effect is captured.

Consider now applying the two-step reduction procedure for case B. Applying the second reduction step (the PR-TBR algorithm) we were able to extract a model with 24 poles that is indistinguishable from the PRIMA-generated 62nd-order model and is therefore a very accurate approximation to the original system. Close examination of the approximation obtained with PRIMA + PR-TBR indicates a very good approximation to the majority of the relevant system poles using a significantly
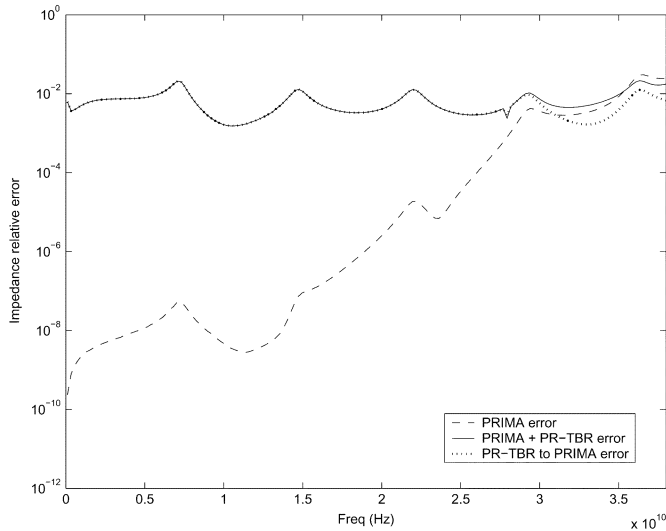
Fig. 7. Results obtained for a simple geometry when skin effect is modeled (case B). Plot shows the errors incurred by the two reduction steps.
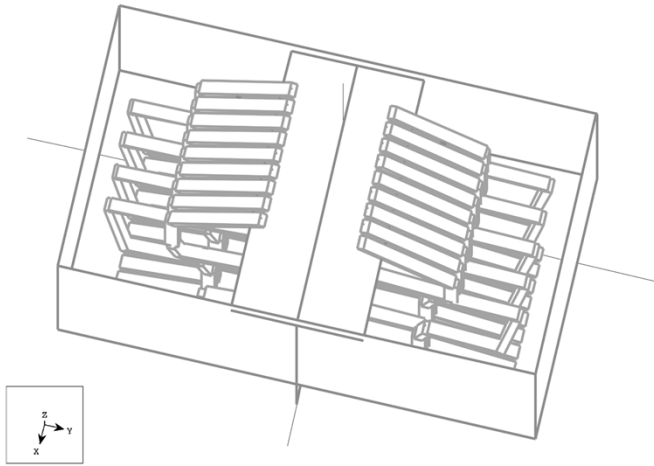

Fig. 8. Three-dimensional connector (courtesy of M. Tsuk, Hewlett-Packard).

smaller order. In Fig. 7, we plot the errors of the various reduction steps as compared to the original full system, as well as the error incurred by the second reduction step alone (with respect to the PRIMA model). Note that the error of the second reduction step, using PR-TBR, is easily controllable. Here, we have chosen to make it less than 1% when compared to the PRIMA model (the phase error is not shown and is also below 1%). This plot proves that the two-step reduction is able to prune the unnecessary model information without significant loss of accuracy. The additional model size reduction is therefore not being obtained at the cost of accuracy degradation. Furthermore, the reduction ratio obtained with the two-step procedure advocated is now close to the reduction obtained with PRIMA in case A without modeling skin effect (for that case, the second step still provided some reduction, albeit very small).

B. Connector Example

For our next example, consider the connector structure in Fig. 8, which consists of 18 pins. The cross section of each pin is 0.25×0.4 mm. Each pin is composed of several straight segments, together reaching a height of 18.5 mm. The pins are enclosed in a box of metallic plates measuring 14.5×8 mm and 11 mm in height and for the dielectric used $\epsilon = 3.5\epsilon_0$. For this experiment, we will limit ourselves to discretizing a subset of the conductor structure consisting of only six adjacent pins. A discretization operation is performed dividing each pin in eight segments along its length, and using a 12-filament (3×4) bundle on each segment, in order to capture skin and proximity effects. Including ground shields, the final PEEC-like circuit has 582 filaments and 864 panels. Using our nodal formulation, we obtain a system with 652 states. To this system we first applied the PRIMA-model reduction algorithm as described in Section III-A, that is only **one** step of the proposed order reduction approach. For this example, and since one wavelength correponds to around 8.7 GHz, we attempted to obtain models which were accurate up to a few gigahertz. We computed, using an expansion at $s_0 = 0$, two approximation models with orders 182 and 420 which were found to be accurate up to 2 GHz and almost 7 GHz, respectively. This is the range of frequencies of interest for this modeling procedure, and for this range of frequencies the EMQS approximation is valid.

However, considering in each case, the frequency range for which the approximation is accurate, it appears that the model sizes required to attain such accuracy are larger than expected. Confirming what was stated for the two-connector case (first example), a pole-residue decomposition operation on both reduced-order models shows that by using only a much smaller set of carefully chosen poles for each model, the frequency responses would be indistinguishable from those presented in the figure. Indeed, after applying our second step of reduction, that is, the PR-TBR algorithm, to the 420 states reduced model presented before, we get a system with 118 states whose frequency response is similar up to the frequency where it was still valid (around 7 GHz). Using the less accurate PRIMA approximation with size 182, and applying the PR-TBR procedure to it, we notice that, in fact, it is possible to obtain an equally accurate approximation using only 67 states. In both cases, the final model order is chosen such that the maximum error between the PRIMA and PRIMA + PR-TBR models is, as we stated, below 2%, which in essence makes the resulting frequency plot undistinguishable.

In Fig. 9, we show the results obtained for the self-impedance of one of these pins. As before, the range of frequencies shown is greater than that valid for the model under the quasistatic approximation (again, one wavelength corresponds to around 8.7 GHz). This range was chosen only for the purpose of illustration from a numerical standpoint. Confirming our expectations, the plot also shows that increasing model size leads to approximations that accurately match the full model response in a larger range of frequencies, starting from the expansion point.

This industrial example again shows that the standard order-reduction schemes (first step of the proposed methodology) are not able to sufficiently compact the models, but the two-step procedure does produce accurate and compact reduced-order models.

C. Multiconductor Structure

Consider now a third structure, a printed circuit board from Teradyne, Inc, shown in Fig. 10. It is made of four thin
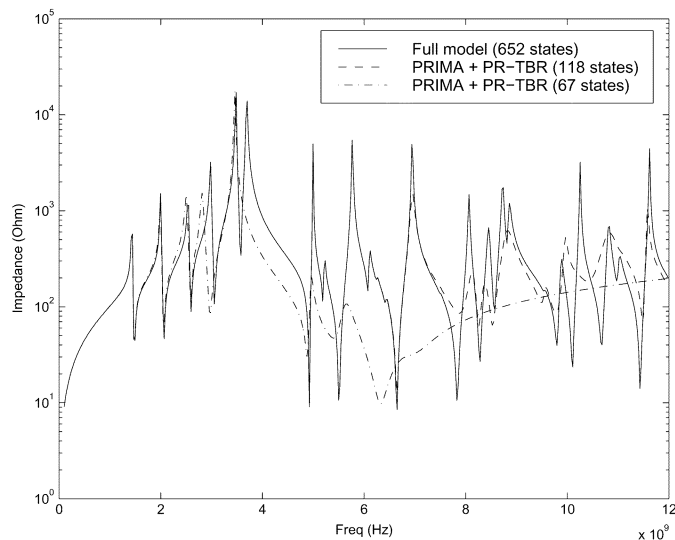
Fig. 9. Various reduced-order models for the connector structure. Original full model and reduced models obtained with PRIMA + PR-TBR of orders 118 and 67. These are indistinguishable from those obtained using only PRIMA reduction of orders 420 and 182 (not shown).
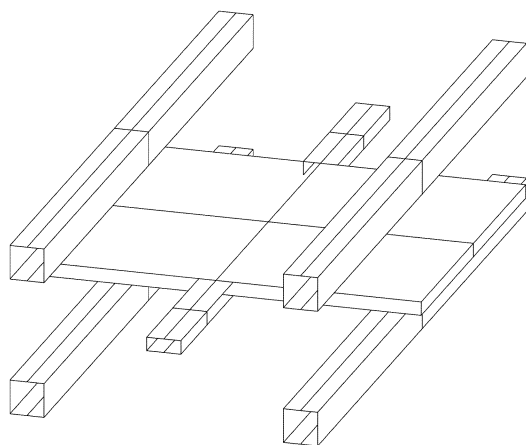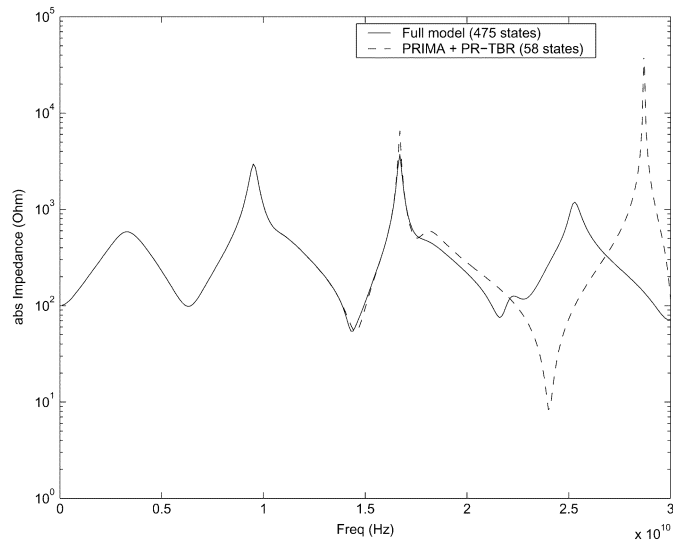

Fig. 10. Printed circuit board connector.

Fig. 11. Results obtained for the Teradyne multiconductor structure using the nodal formulation. Comparisons are made between the full model and a 252nd-order model computed using an expansion point at $s_0 = 0$. The figure also shows the impedance frequency response.

TABLE I
COMPARISON OF EFFICIENCY OF PROPOSED MODELING TECHNIQUES.
RELEVANT FEATURES FOR THE VARIOUS EXAMPLES AS WELL AS THE
ORDER OF THE VARIOUS MODELS OBTAINED

Example	# filaments	# panels	Full Model	PRIMA	PRIMA + PR-TBR
Tline (case B)	150	416	323	62	24
Connector (I)	582	864	652	182	67
Connector (II)	582	864	652	420	118
Teradyne	330	1326	475	252	58

reductions are possible with the proposed two-step algorithm without any loss of accuracy.

D. Summary and Time-Domain Results

Table I presents a summary of the examples discussed in this paper. Included are the relevant features of each geometry, the sizes of the full models, the model obtained after reduction by PRIMA alone, and the reduced model obtained by the two-step procedure proposed in this paper. Each pair of reductions for each model is computed for the same precision. It can be seen that while PRIMA alone is sometimes not as effective as one would want or expect, the two-step combination of using PRIMA followed by PR-TBR is able to obtain an additional 60 to 75% improvement without incurring any significant accuracy penalty.

Finally, in Fig. 12, we present a comparison between results of a time-domain simulation obtained with a reduced model generated with our formulation and experimental measurements. For this experiment, we used the subset of the connector presented previously in Section IV-B with all pins connected to ground through resistors. Then a noisy input is connected in series with one of these resistors and a step with a 500-ps rise-time is imposed on it. Typically, the EMQS model is valid if the signal's rise time is greater than twice (two way trip) the propagation time (time for the signal to reach the end of the connector). In this case, the rise time is 5 ps, and the propagation time is $1/8.7 \times 10^9 = 0.115$ ps, and so, the EMQS

conductors placed along a central conductor which assumes a planar geometry in the middle part. Fifty-ohm resistances connect each pin to the middle one on one side. At the other end, the impedance is computed between one pin and the central one. This structure was previously studied in [35] to show the importance of 3-D effects, comparing a 2-D analysis based on transmission line theory with our 3-D formulation. A discretization in 330 filaments and 1326 panels is now performed on this structure, which models skin effect, resulting in a system with 475 states. Applying the PRIMA algorithm, again with an expansion point of $s_0 = 0$, we obtain a reduced model which still has 252 states. By applying the PR-TBR algorithm to this reduced PRIMA model, we achieve the same precision, up to the same frequency, using a model with only 58 states (the error between the two reduced-order models is below 1%). As can be seen in Fig. 11, these reduced models are valid up to around 14 GHz. Since one wavelength corresponds to 15 GHz, assuming the speed of light, this is clearly a model for which the EMQS approximation is valid. Again, significant
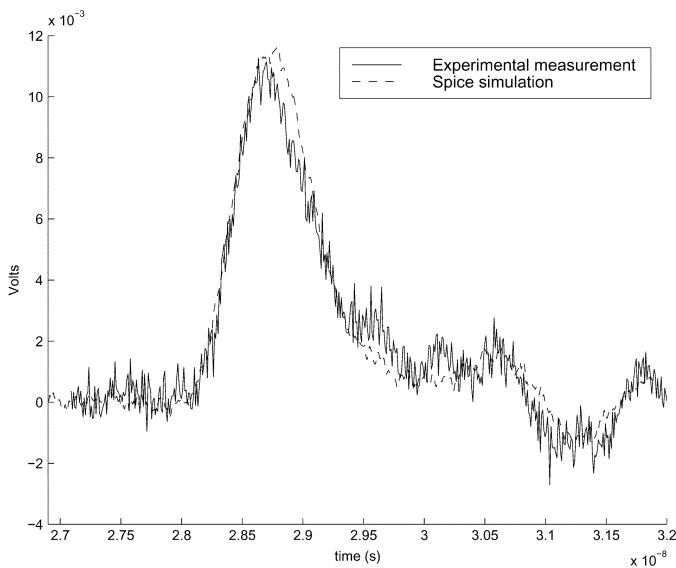
Fig. 12. Comparison between measured time-domain waveforms and simulated results obtained using a reduced-order model of the connector example.

approximation is acceptable. Applying the input waveform to the resulting model and collecting the voltage waveform at an adjacent pin results in the plot shown. As can be seen from the plot, the waveforms are qualitatively similar and acceptable accuracy is obtained. If higher accuracy is required, a finer discretization can be used. The plot shown here was obtained using the approximation computed with the two-step approach. Similar results for the PRIMA reduced model alone were presented previously in [4]. The waveforms in both cases are indistinguishable (as expected since the only difference between the two model is due to the existance in the PRIMA approximation of poles with negligible residues which have no relevance for the time response). The example shows therefore that both models, computed either with PRIMA solely or with PRIMA+PR-TBR are time-domain accurate and guaranteed passive. The two step-method proposed in this paper, however, besides accurate and passive, is also more efficient as it results in a more compact model.

V. CONCLUSION

The main contribution of this paper is the presentation of a new modeling approach for efficiently generating accurate, compact, guaranteed passive reduced-order models of circuit and packaging interconnects. The approach relies on a nodal or mixed nodal-mesh PEEC-like formulation which is then combined with a two-step model order reduction procedure. The nodal and mixed nodal-mesh formulations have advantages over previously published formulations since they produce models with fewer states, provide for increased flexibility in the order-reduction techniques, and lead in general to better conditioned systems. The order reduction procedure presented is a two-step method consisting of a Krylov-subspace moment-matching process followed by a nearly optimal positive-real truncated balanced realization algorithm. The

proposed approach allows for the efficient generation of reduced-order models of 3-D interconnect structures and was shown to improve the efficiency of parasitic extraction and coupled simulation of circuits and interconnects. The formulation and model-order reduction method were used to demonstrate, for several industrial examples, extraction of parasitics models whose accuracy was validated against measured time-domain data.

REFERENCES

[1] K. Nabors, S. Kim, and J. White, "Fast capacitance extraction of general three-dimensional structures," *IEEE Trans. Microwave Theory Tech.*, vol. 40, pp. 1496–1506, July 1992.

[2] M. Kamon, M. J. Tsuk, and J. White, "Fasthenry: A multipole-accelerated 3-D inductance extraction program," *IEEE Trans. Microwave Theory Tech.*, vol. 42, pp. 1750–1758, Sept. 1994.

[3] M. Kamon, "Fast parasitic extraction and simulation of three-dimensional interconnect via quasistatic analysis," Ph.D. Dissertation, Mass. Inst. Technol., Cambridge, MA, Jan. 1998.

[4] N. Marques, M. Kamon, J. White, and L. M. Silveira, "An efficient algorithm for fast parasitic extraction and passive order reduction of 3-D interconnect models," in *Proc. DATE—Design, Automation, and Test in Europe, Exhibition, Conf.*, Paris, France, Feb. 1998, pp. 538–548.

[5] ——, "A mixed nodal-mesh formulation for efficient extraction and passive reduced-order modeling of 3-D interconnects," in *Proc. 35th ACM/IEEE Design Automation Conf.*, San Francisco, CA, USA, June 1998, pp. 297–302.

[6] A. E. Ruehli, "Equivalent circuit models for three-dimensional multiconductor systems," *IEEE Trans. Microwave Theory Tech.*, vol. MTT-22, pp. 216–221, Mar. 1974.

[7] ——, "Circuit oriented electromagnetic solutions in the time and frequency domain," *IEICE Trans. Commun., Special Issue EMC Implications Densely Mounted Electronic Devices*, vol. E80-B, no. 11, pp. 1594–1603, Nov. 1997.

[8] H. Heeb and A. E. Ruehli, "Three-dimensional interconnect analysis using partial element equivalent circuits," *IEEE Trans. Circuits Syst. I*, vol. 39, pp. 974–982, Nov. 1992.

[9] A. E. Ruehli and H. Heeb, "Circuit models for three-dimensional geometries including dieletrics," *IEEE Trans. Microwave Theory Tech.*, vol. 40, pp. 1507–1516, July 1992.

[10] L. T. Pillage and R. A. Rohrer, "Asymptotic waveform evaluation for timing analysis," *IEEE Trans. Computer-Aided Design*, vol. 9, pp. 352–366, Apr. 1990.

[11] P. Feldmann and R. W. Freund, "Efficient linear circuit analysis by Padé approximation via the Lanczos process," *IEEE Trans. Computer-Aided Design*, vol. 14, pp. 639–649, May 1995.

[12] L. M. Silveira, M. Kamon, and J. K. White, "Efficient reduced-order modeling of frequency-dependent coupling inductances associated with 3-d interconnect structures," in *Proc. 32nd Design Automation Conf.*, San Francisco, CA, June 1995, pp. 376–380.

[13] K. J. Kerns, I. L. Wemple, and A. T. Yang, "Stable and efficient reduction of substrate model networks using congruence transforms," in *Proc. IEEE/ACM Int. Conf. Computer-Aided Design*, San Jose, CA, Nov. 1995, pp. 207–214.

[14] E. Chiprout and M. S. Nakhla, "Analysis of interconnect networks using complex frequency hopping (CFH)," *IEEE Trans. Computer-Aided Design*, vol. 14, pp. 186–200, Feb. 1995.

[15] L. M. Silveira, M. Kamon, I. Elfadel, and J. K. White, "A coordinate-transformed Arnoldi algorithm for generating guaranteed stable reduced-order models of rlc circuits," in *Proc. Int. Conf. Computer Aided-Design*, San Jose, CA, Nov. 1996, pp. 288–294.

[16] A. Odabasioglu, M. Celik, and L. Pileggi, "PRIMA: Passive reduced-order interconnect macromodeling algorithm," in *Proc. Int. Conf. Computer Aided-Design*, San Jose, CA, Nov. 1997, pp. 58–65.

[17] I. M. Elfadel and D. L. Ling, "A block rational arnoldi algorithm for multipoint passive model-order reduction of multiport rlc networks," in *Proc. Int. Conf. Computer Aided-Design*, San Jose, CA, Nov. 1997, pp. 66–71.

[18] J. Cullum, A. E. Ruehli, and T. Zhan, "A method for reduced-order modeling and simulation of large interconnect circuits and its application to peec models with retardation," *IEEE Trans. Circuits Syst. II*, vol. 47, pp. 261–273, Apr. 2000.

[19] K. Gallivan, E. Grimme, and P. V. Dooren, "Asymptotic waveform evaluation via a Lanczos method," *Appl. Math. Lett.*, vol. 7, no. 5, pp. 75–80, 1994.

[20] L. Greengard and V. Rokhlin, "A fast algorithm for particle simulations," *J. Computational Phys.*, vol. 73, no. 2, pp. 325–348, Dec. 1987.

[21] J. R. Phillips, "Error and complexity analysis for a collocation-grid-projection plus precorrected-FFT algorithm for solving potential integral equations with Laplace or Helmholtz kernels," in *Proc. 7th Copper Mountain Conf. Multigrid Methods*, vol. CP 3339, N. D. Melson, T. A. Manteuffel, S. F. McCormick, and C. C. Douglas, Eds., Hampton, VA, 1996, pp. 673–688.

[22] M. Kamon, N. Marques, L. M. Silveira, and J. White, "Generating reduced-order models via peec for capturing skin and proximity effects," in *Proc. 6th Topical Meeting Electrical Performance Electronic Packaging*, San Jose, CA, Oct. 1997, pp. 259–262.

[23] B. Moore, "Principal component analysis in linear systems: Controllability, observability, and model reduction," *IEEE Trans. Automat. Contr.*, vol. AC-26, pp. 17–32, Feb. 1981.

[24] K. Glover, "All optimal Hankel-norm approximations of linear multivariable systems and their l^∞-error bounds," *Int. J. Control*, vol. 39, no. 6, pp. 1115–1193, June 1984.

[25] L. Pernebo and L. M. Silverman, "Model reduction via balanced state space representations," *IEEE Trans. Automat. Contr.*, vol. AC-27, pp. 382–387, Apr. 1982.

[26] M. Kamon, F. Wang, and J. White, "Generating nearly optimally compact models from Krylov-subspace based reduced-order models," *IEEE Trans Circuits Syst. II*, vol. 47, pp. 239–248, Apr. 2000.

[27] L. M. Silveira, N. Marques, M. Kamon, and J. White. Improving the efficiency of parasitic extraction and simulation of 3-D interconnect models. presented at ICECS'99—IEEE Int. Conf. Electronics, Circuits, and Systems. [Online]. Available: http://algos.inesc.pt/~lms/publications/icecs99-mor.ps.gz

[28] J. Phillips, L. Daniel, and L. M. Silveira, "Guaranteed passive balancing transformations for model order reduction," *IEEE Trans. Computer-Aided Design*, vol. 22, pp. 1027–1041, Aug. 2003.

[29] C. Desoer and E. Kuh, *Basic Circuit Theory*. New York: McGraw-Hill, 1969.

[30] T. V. Nguyen, J. Li, and Z. Bai, "Dispersive coupled transmission line simulation using an adaptive block lanczos algorithm," in *Proc. Int. Custom Integrated Circuits Conf.*, 1996, pp. 457–460.

[31] L. M. Silveira, I. M. Elfadel, J. K. White, M. Chilukura, and K. S. Kundert, "Efficient frequency-domain modeling and circuit simulation of transmission lines," *IEEE Trans. Comp., Packaging, Manufact. Technol. B*, vol. 17, pp. 505–513, Nov. 1994.

[32] C. P. Coelho, J. R. Phillips, and L. M. Silveira, "A convex programming approach for generating guaranteed passive approximations to tabulated frequency-data," *IEEE Trans. Computer-Aided Design*, vol. 23, pp. 293–301, Feb. 2004.

[33] ——, Robust rational function approximation algorithm for model generation. presented at 36th ACM/IEEE Design Automation Conf. [Online]. Available: http://algos.inesc.pt/~lms/publications/dac99-interp.ps.gz

[34] M. Kamon, N. Marques, and J. White, "FastPep: A fast parasitic extraction program for complex three-dimensional geometries," in *Proc. Int. Conf. Computer Aided-Design*, San Jose, CA, Nov. 1997, pp. 456–460.

[35] N. C. Marques, "Efficient algorithms for extraction and passive order-reduction of 3-D interconnect Models," M.S. Thesis, Elect. Comput. Eng., Instituto Superior Técnico, Tech. Univ. Lisbon, Lisbon, Portugal, Jan. 1998.

[36] Y. Saad and M. H. Schultz, "GMRES: A generalized minimal residual algorithm for solving nonsymmetric linear systems," in *SIAM J. Scientific Statistical Computing*, vol. 7, July 1986, pp. 856–869.

[37] M. Kamon, "Efficient techniques for inductance extraction of complex 3-D geometries," M.S. Thesis, Mass. Inst. Technol., Cambridge, MA, Feb. 1994.

[38] B. D. Anderson and S. Vongpanitlerd, *Network Analysis and Synthesis*. Englewood Cliffs, NJ: Prentice-Hall, 1973.

[39] L. N. Trefethen and D. Bau, *Numerical Linear Algebra*. Philadelphia, PA: SIAM, 1997.

Nuno Alexandre Marques was born in Lisbon, Portugal. He received the Engineer's degree in electrical and computer engineering in 1995 from the Instituto Superior Técnico, the Technical University of Lisbon and the M.S. degree, also in electrical and computer engineering, from Instituto Superior Técnico in 1998. His Master's thesis was entitled "Efficient Algorithms for Extraction and Passive Order-Reduction of 3-D Interconnect Models."

His research interests are in the area of algorithms and techniques for three-dimensional modeling and simulation of electromagnetic field effects in interconnects and package structures. He is presently working in the field of mobile communications technology.

Mattan Kamon received the B.S. degree in engineering science and the M.A. degree in mathematics in 1991 from the Pennsylvania State University, University Park, and the M.S. and Ph.D. degrees in electrical engineering and computer science in 1994 and 1998, respectively, from the Massachusetts Institute of Technology, Cambridge. For his graduate work, he developed efficient algorithms for 3-D interconnect parameter extraction and simulation.

He joined Microcosm Technologies, later Coventor, Inc., after graduation, where he has developed CAD tools for fast inductance and magnetic force calculation for package analysis and microelectromechanical system (MEMS) design.

Luís Miguel Silveira (S'85–M'95) was born in Lisbon, Portugal. He received the Engineer's degree (summa cum laude) in 1986 and the M.S. degree in electrical and computer engineering in 1989, both from the Instituto Superior Técnico, Technical University of Lisbon and the M.S., E.E., and Ph.D. degrees in 1990, 1991, and 1994, respectively, from the Massachusetts Institute of Technology, Cambridge. His doctoral dissertation was entitled "Model Order Reduction Techniques for Circuit Simulation." From 1992 to 1994, he was supported by an IBM doctoral fellowship.

He is currently an Associate Professor at the Instituto Superior Técnico (IST), Technical University of Lisbon, a Senior Researcher in the Electronics Division of the Instituto de Engenharia de Sistemas e Computadores (INESC-ID), Lisbon, Portugal, and a founding member of the Lisbon Center of the Cadence Laboratories. His research interests are in various aspects of computer-aided design of integrated circuits with emphasis on parallel computer algorithms and the theoretical and practical issues concerning numerical simulation methods for circuit design problems.

Jacob K. White (S'80–M'83) received the B.S. degree in electrical engineering and computer science from Massachusetts Institute of Technology (MIT), Cambridge, in 1980 and the S.M. degree and the Ph.D. degree in electrical engineering and computer science from the University of California, Berkeley, in 1983 and 1985, respectively.

He is currently with MIT, where he is a Professor in electrical engineering and computer science and an Associate Director of the Research Laboratory of Electronics. He previously worked at the IBM T. J. Watson Research Center, Yorktown Heights, NY, from 1985 to 1987 and was the Analog Devices Career Development Assistant Professor at MIT from 1987 to 1989. His current research interests are in numerical algorithms for problems in circuits, interconnect, micromachined devices, and biological systems.

Dr. White was an Associate Editor of the IEEE TRANSACTIONS ON COMPUTER-AIDED DESIGN from 1992 until 1996, was chair of the International Conference on Computer-Aided Design in 1999, and was a 1988 Presidential Young Investigator.